Electronic Supplementary Material (ESI) for Dalton Transactions.

Supporting Information

Protonation effect on ligands in EuL: a luminescent switcher for fast naked-eye detection of HCl

Jun Zhang, Wen-Bin Yang, Xiao-Yuan Wu, Xiao-Fei Kuang, and
Can-Zhong Lu*

Key Laboratory of Design and Assembly of Functional

Nanostructures, Fujian Institute of Research on the Structure of

Matter, Chinese Academy of Sciences Fuzhou, Fujian 350002 (China)

*E-mail: czlu@fjirsm.ac.cn

1. Experimental detail

1) Materials

All of the chemicals were obtained from commercial sources and used without further purification. The ligand H**L** (H**L**=2-(2-Pyridin-2-yl)quinoline-4-carboxylic acid) was synthesized according to the procedure described previously.[1]

2) Method

Elemental Analysis. The elemental analysis were performed on an EA1110 CHNS-0 CE elemental analyzer.

FT-IR Spectroscopy. The IR spectra were recorded on a PECO (U.S.A.) SpectrumOne spectrophotometer with KBr pellets 4000-500cm^{-1}.

TGA Analysis. Thermal stability studies were carried out on a TGA/DSC 1 STAR^{e} system with a heating rate of 10 °C/min, from 30°C to 1000°C in N_2.

UV–Vis Spectroscopy. The UV/Vis spectra were recorded on a Varian Cary 500 Scan UV/Vis system.

Powder X-Ray Diffraction. The phase purity and crystallinity of each product were checked by PXRD using a Rigaku Miniflex2 diffractometer with Cu-Kα radiation (λ=1.54056 Å).

NMR spectra. ^{1}H NMR spectra were recorded on a Bruker Avance III 400 MHz NMR spectrometer.

Photoluminescence Measurements. Photoluminescence spectra at

10K were recorded on an Edinburgh Analytical instrument FLS920. The time-dependent fluorescence quenching profiles were measured by an luminescence experimental sensor setup reported by sun group[2].

The changes of emission intensity were used for detection signal after the **EuL** sample exposure to HCl vapor. For Figure 3 in the main text, luminescence decreases for HCl vapor was measured at different times. As showed in Figure S1, powder samples of **EuL** (50mg) were pressed into firm sheet sample and sticked to the quartz slide by a double-sided black conductive adhesive, far from the bottom side of quartz cuvette about 1.5 cm. The length and width are 1 cm, the height is 4.2 cm for the quartz cuvette, which matchs the solid sample holder of Edinburgh Analytical instrument FLS920. The quartz slide is 1.2 cm ×3.5 cm, whose width is equal to the diagonal distance of quartz cuvette.

The solid state emission spectrum of firm sheet sample is carried out and as an original standard, then 200 uL concentrated hydrochloric acid (37% HCl solution) are added into the bottom of cuvette by toppette pipettor. The cuvette must be kept still in all over the process. Replace the cap of the cuvette and record the luminescence spectra and intensity as well as the response of the sensor slide versus time in HCl vapor. Similar test method was used to obtain the time-dependant PL spectra of **EuL-HCl** upon exposure to NH_3 vapor at room temperature, with instead of 200 uL strong ammonia.

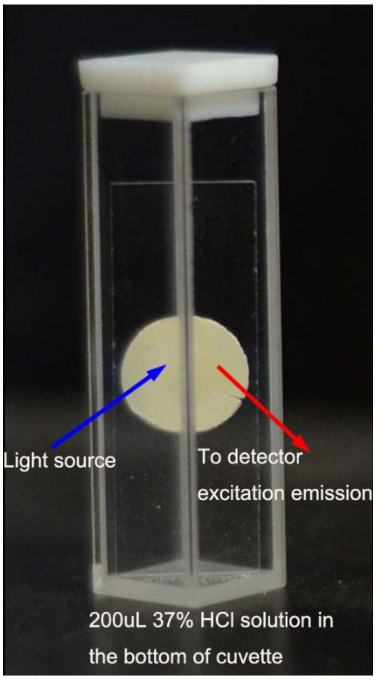

Figure S1. Diagram of gas-sensing measurements for HCl vapor.

Single-Crystal X-Ray Crystallography. Diffraction data of **EuL** and **$H_2LCl·H_2O$** were collected on a SuperNova, Dual, Cu/Mo at zero, Atlas diffractometer equipped with graphite-monochromated Cu/Mo Kα radiation (λ_{Cu} =1.54184 Å, λ_{Mo} =0.71073 Å). Diffraction data of **TbL** was collected on a Rigaku Mercury and a Saturn724 CCD diffractometer equipped with graphite-monochromated Mo Kα radiation (λ=0.71073 Å). Structures were solved by direct methods and refined by full-matrix least-squares methods with SHELXL-97 program package[3]. Hydrogen atoms were added in idealized positions except hydrogen atoms of water in compound **$H_2LCl·H_2O$**, which was located from difference maps and refined freely. All nonhydrogen atoms were refined anisotropically. Details of crystal and structure refinement are listed in Table S1. CCDC 1055165, 1055166, and 1055167 contain the supplementary crystallographic data for compounds **EuL**, **TbL**, and **$H_2LCl·H_2O$**, respectively.

Computational Section

The electronic excitation states were computed by using time-dependent Hartree-Fock method (TDHF), followed by a Møller-Plesset correlation energy correction truncated at second-order (MP2) at the 6-311G* basis set level. The energy convergence of 10-7a.u. was set for the excited states.

3) **Synthesis**

Synthesis of compounds EuL and EuL

$EuH(\mathbf{L})_2(NO_3)_2$ (**EuL**). A mixture of $Eu(NO_3)_3·6H_2O$ (44.6mg, 0.1 mmol), H**L**(25m g, 0.1 mmol), CH_3CN (10ml) was stirred in a stainless steel autoclave with a Teflon-liner, then the mixture was heated at 100 °C for 72 hours. After this period the autoclave was slowly cooled to room temperature and the yellow crystals were washed several times with CH_3CN, filtered and dried. The yield of the reaction was 60 %, based on H**L**. Elemental analysis calcd (%) for $EuC_{30}H_{19}N_6O_{10}$: C 46.46, H 2.47, N 10.84; found: C 46.43, H 2.62, N 11.07.

$TbH(\mathbf{L})_2(NO_3)_2$ (**TbL**). The compound **TbL** was prepared by the same procedure as for compound **EuL**, but with $Tb(NO_3)_3 \cdot 6H_2O$ (45.3mg, 0.1 mmol). The yield of compound **TbL** was 64%, based on H**L**. Elemental analysis calcd (%) for $TbC_{30}H_{19}N_6O_{10}$: C 46.05, H 2.45, N 10.74; found: C 45.28, H 2.56, N 10.38.

Synthesis of $H_2LCl \cdot H_2O$

50 mg H**L** was dissolved in 5 mL of 37% HCl solution, after filtration, the filtrate was left for slow evaporation at room temperature. Yellow needle crystals were obtained after 48 hours. A single phase was obtained in 53% yield. The presence of a unique phase was confirmed by PXRD (Figure S2) and elemental analyses. Calcd (%) for $C_{15}H_{13}ClN_2O_3$: C, 59.12; H, 4.30; N, 9.19. Found (%): C, 58.87; H, 4.37; N, 9.33.

EuL-HCl from treatment of EuL with HCl vapor Upon exposure to HCl vapor at room temperature for 300s, the emission of **EuL** was quenched completely.

EuL-NH_4Cl from treatment of EuL-HCl with NH_3 vapor Upon exposure to NH_3 vapor at room temperature for 90s, the fluorescence of **EuL-HCl** enhancing reaches a maximum.

2. Analyses information

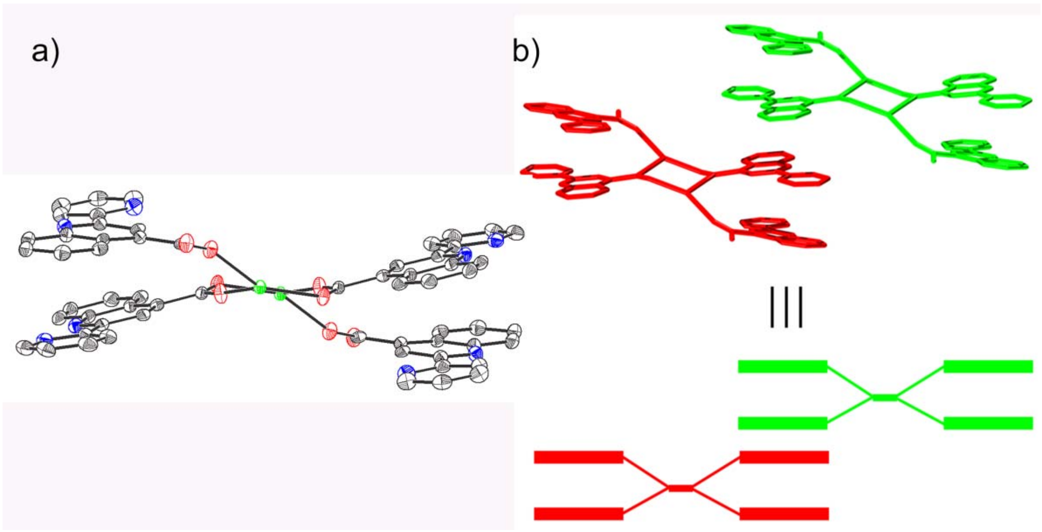

Figure S2. a) tweezer-type SBU of **EuL**; b) tweer-type SBU structure of EuL and π−π stacking interactions between adjacent SBUs. C, black; O, red; N, blue; Eu, green; all hydrogen atoms and nitrate are omitted for clarity.

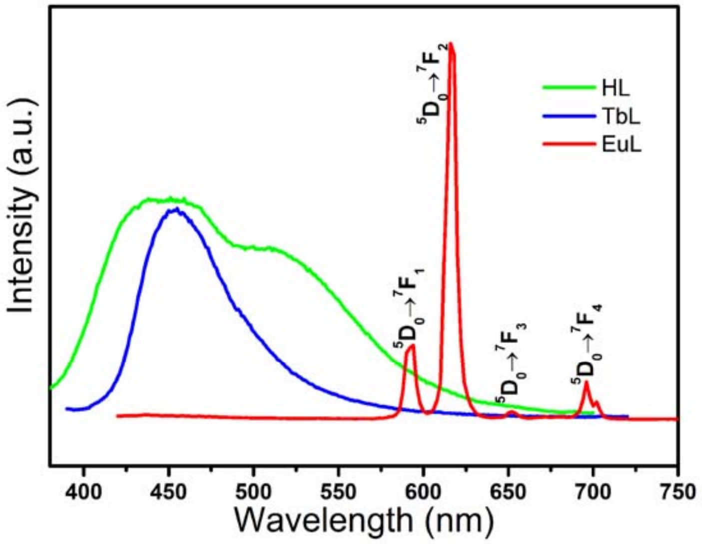

Figure S3. Room temperature emission spectra for H**L**, **TbL**, and **EuL** excitation at 360nm, 370nm, 395nm, respectively.

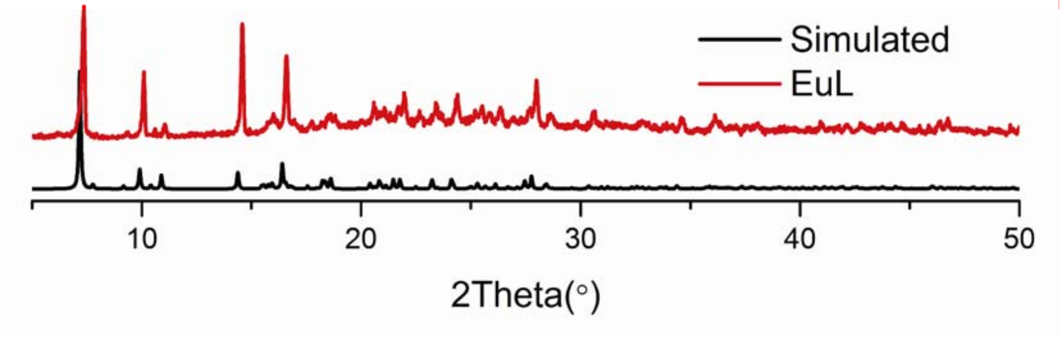

Figure S4. Powder X-ray diffraction patterns of compound **EuL**.

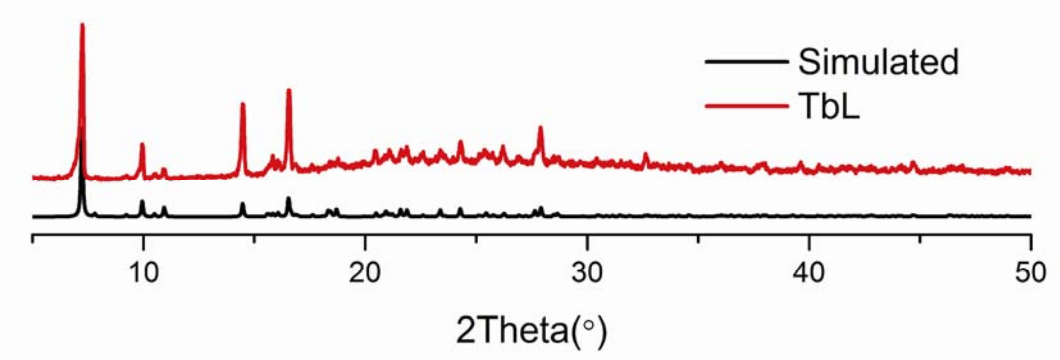

Figure S5. Powder X-ray diffraction patterns of compound **TbL**.

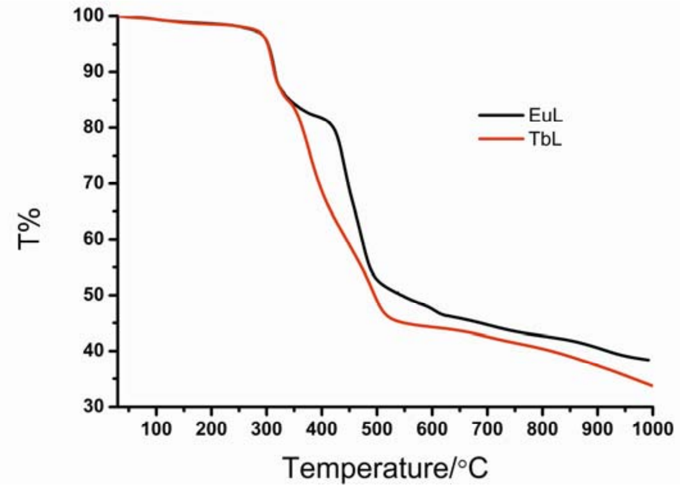

Figure S6. TGA profile of compound **EuL** and **TbL** in temperature range of 30 – 1000 °C under nitrogen atmosphere.

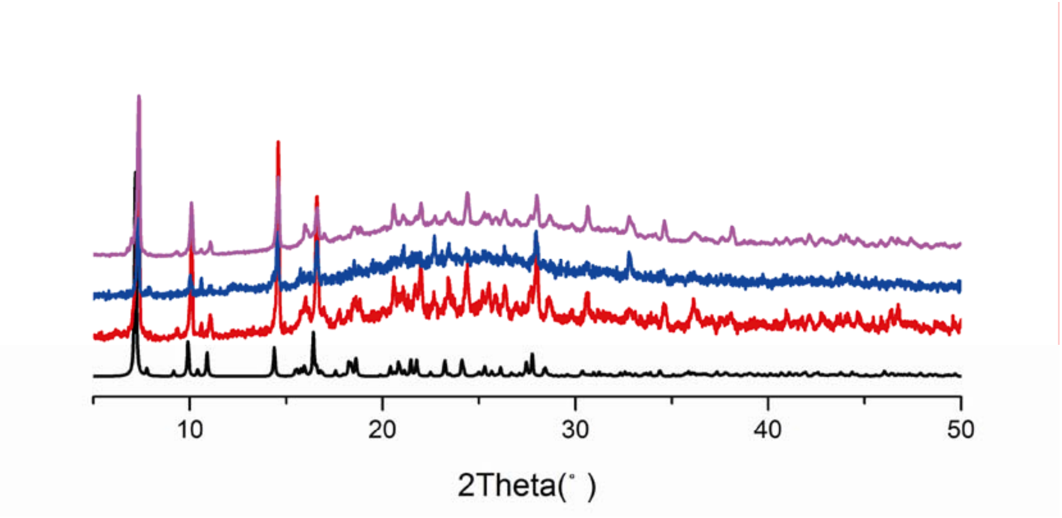

Figure S7. Powder X-ray diffraction patterns of **EuL**-related systems. Black, simulated PXRD of **EuL**. Red, original **EuL** sample. Blue, **EuL-HCl**. Purple, **EuL-NH$_4$Cl**.

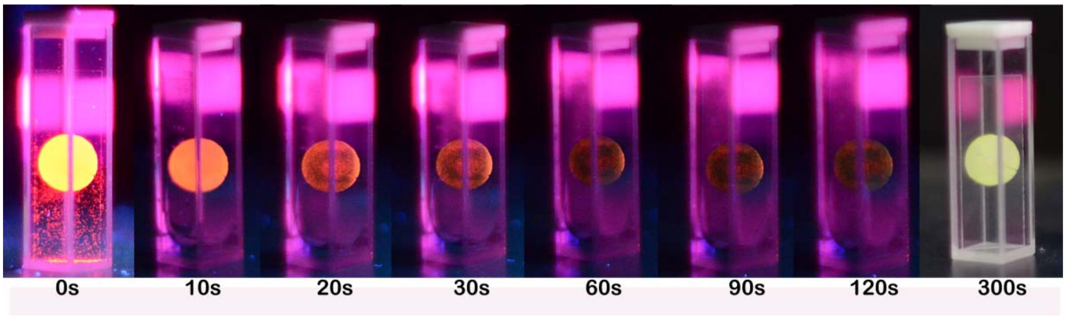

Figure S8. Photographs of the fluorescence intensity changes of **EuL** emission after exposure to HCl vapor at various time intervals under 365 nm ultraviolet at room temperature.

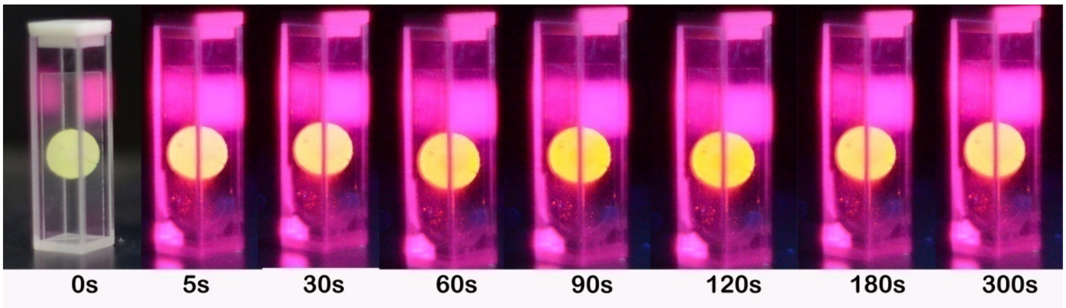

Figure S9: Photographs of the fluorescence intensity changes of the **EuL-HCl** sheet upon exposure to NH_3 vapor at various time intervals under 365 nm ultraviolet at room temperature.

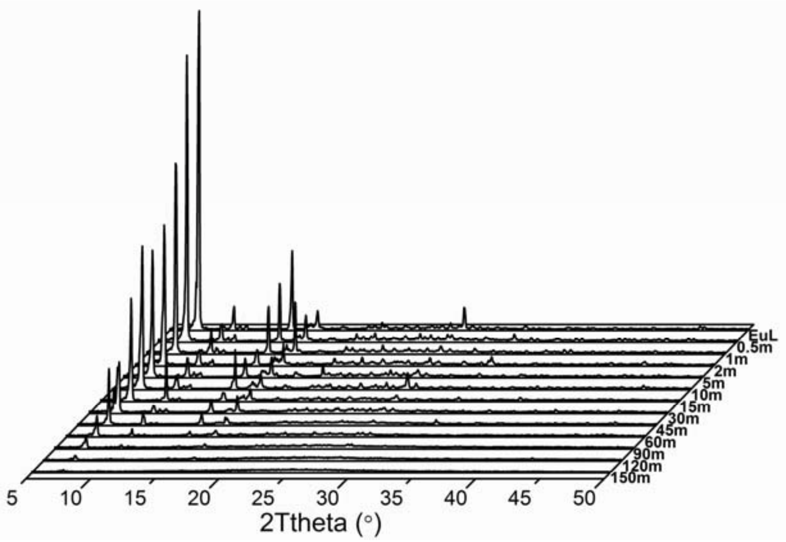

Figure S10. Time-dependant PXRD patterns of **EuL** upon exposure to HCl vapor at room temperature.

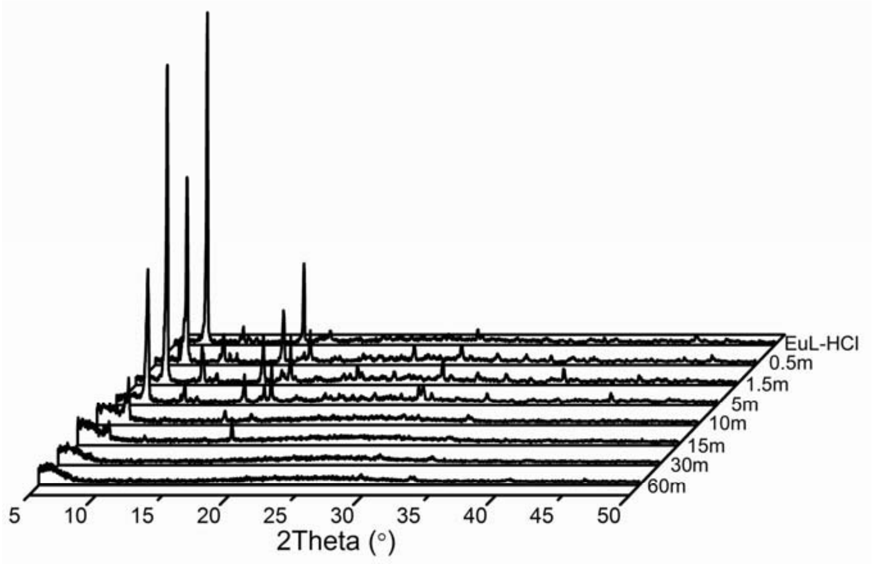

Figure S11. Time-dependant PXRD patterns of **EuL-HCl** upon exposure to NH_3 vapor at room temperature.

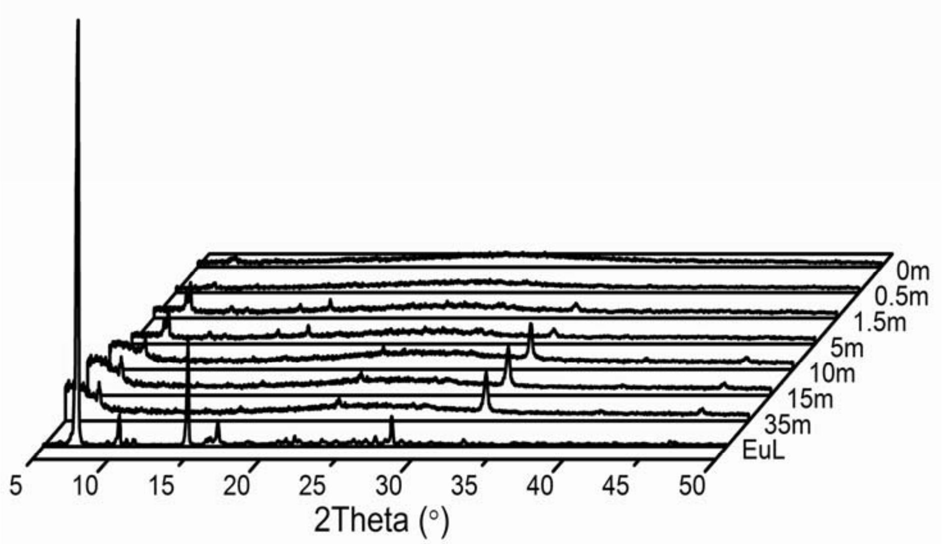

Figure S12. Time-dependant PXRD patterns of **EuL** which treat with HCl vapor over one hour and frameworks collapse upon exposure to NH_3 vapor at room temperature.

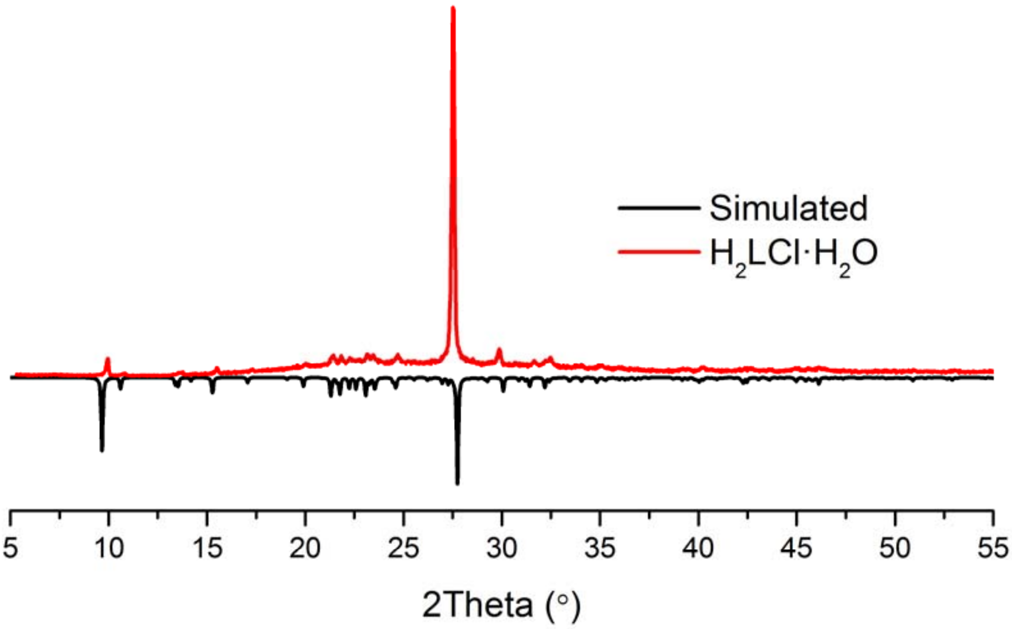

Figure S13: Powder X-ray diffraction patterns of compound **$H_2LCl\cdot H_2O$**.

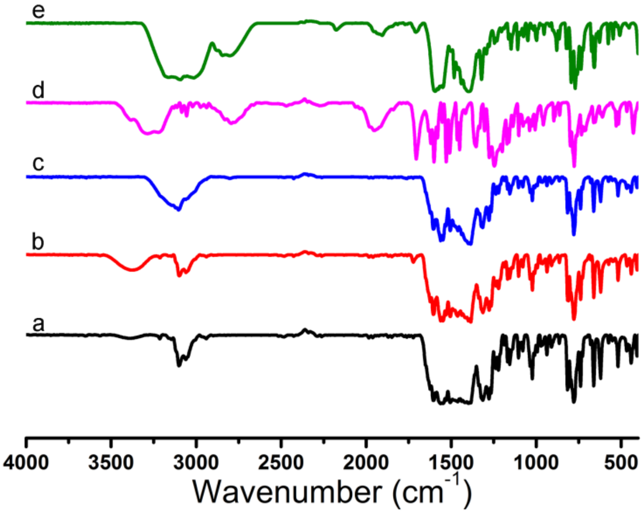

Figure S14. FT-IR spectra of **EuL**-based systems and **$H_2LCl\cdot H_2O$** systems.

a **EuL**, b **EuL-HCl**, c **EuL-NH_4Cl**, d **$H_2LCl\cdot H_2O$**, e **$H_2LCl\cdot H_2O$-NH_3**.

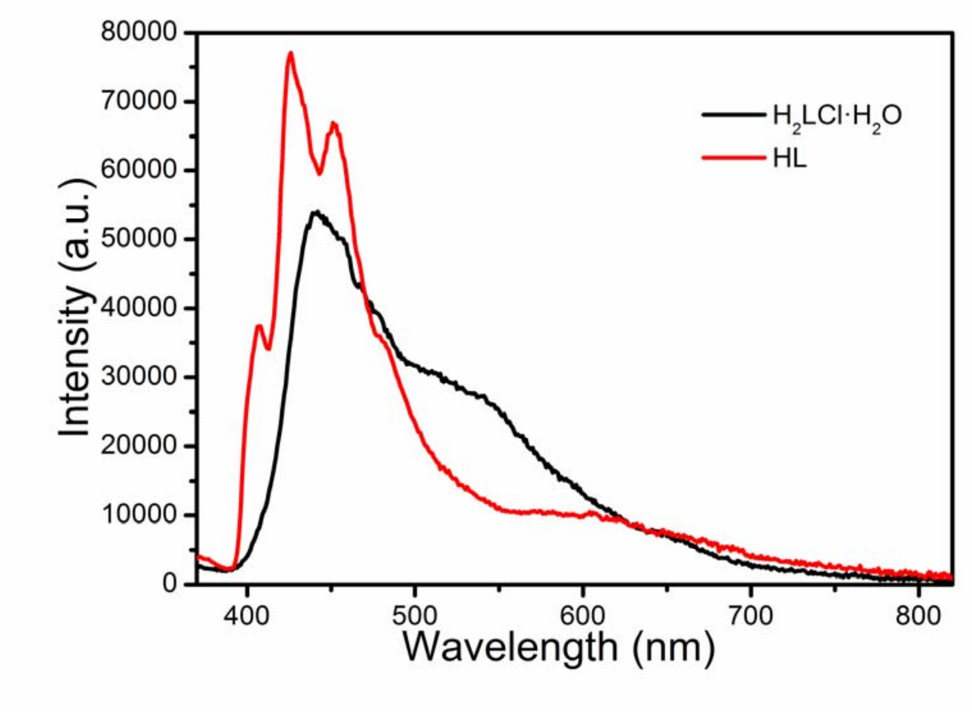

Figure S15. Low Temperature (10K) Emission Spectra of H**L** and

$\mathbf{H_2LCl\cdot H_2O}$.

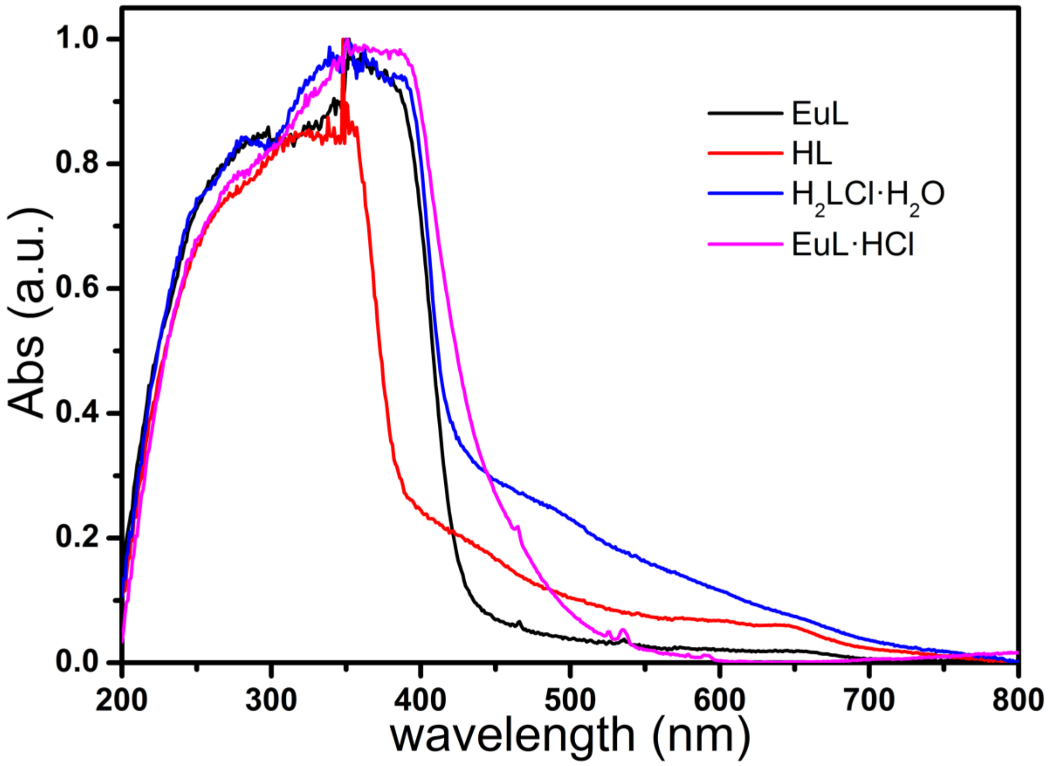

Figure S16. UV/Vis diffuse reflectance spectra.

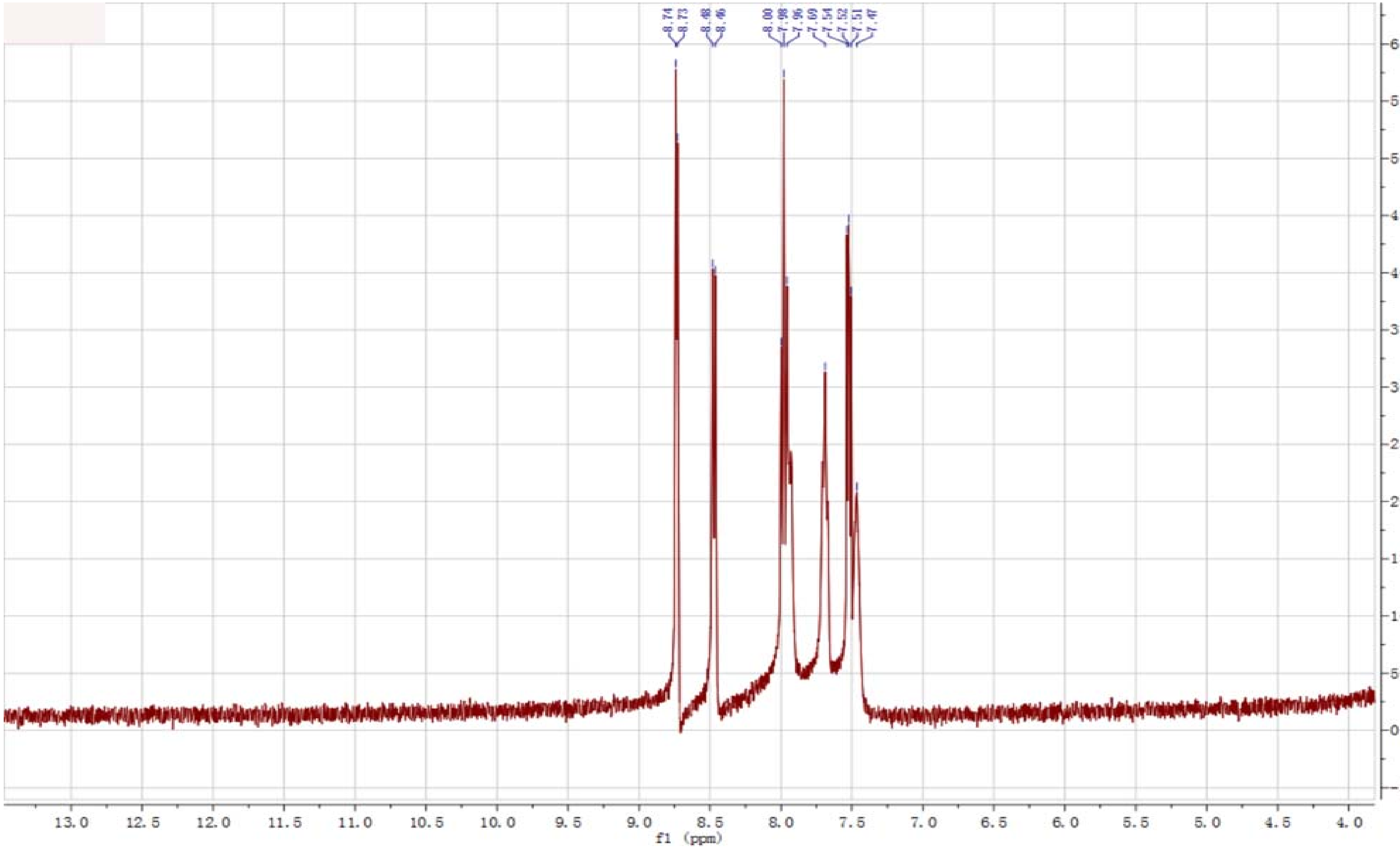

Figure S17. ^{1}H-NMR of **EuL** dissolved inDMSO-d^6.

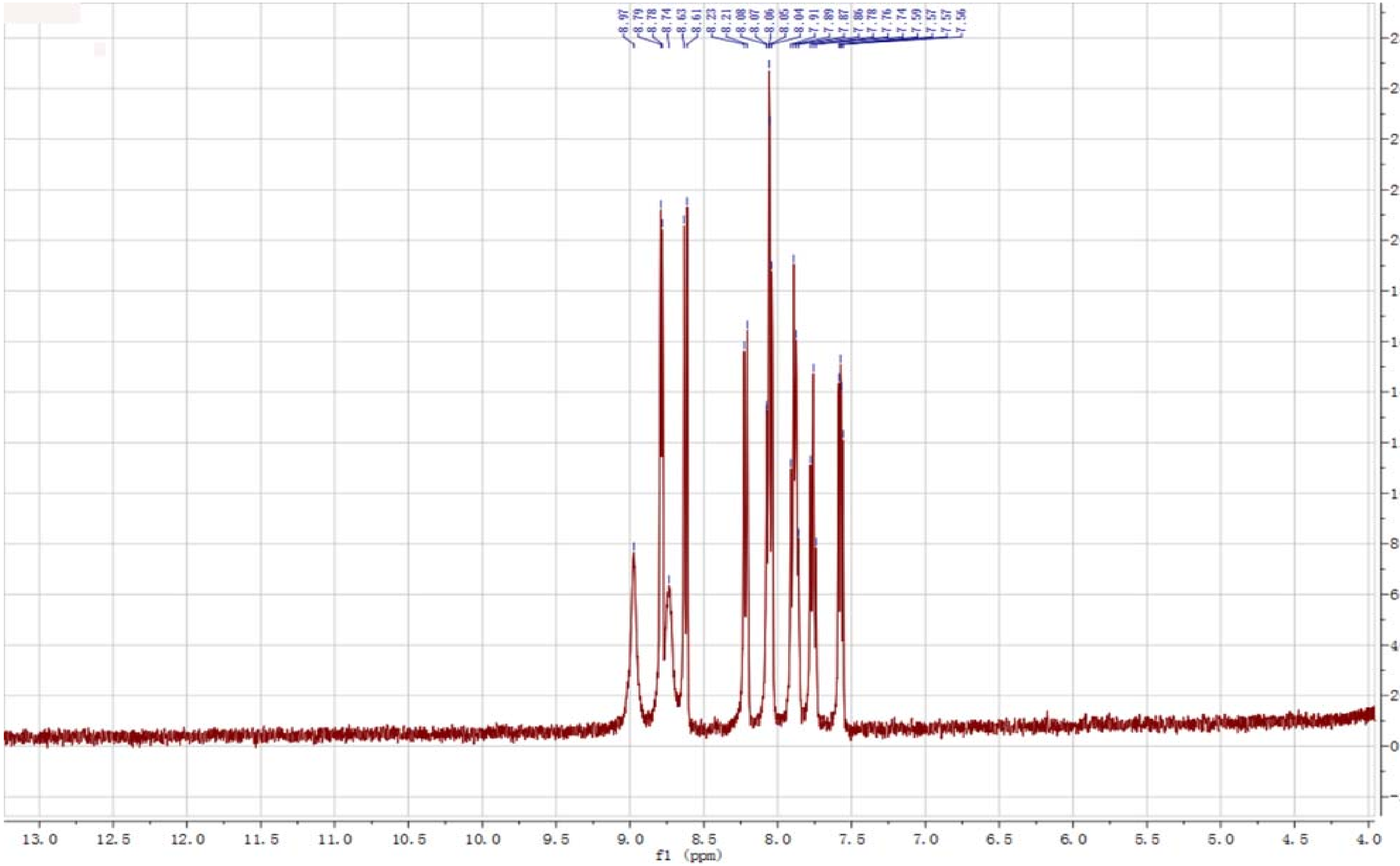

Figure S18. ^{1}H-NMR of **EuL-HCl** dissolved inDMSO-d^{6}.

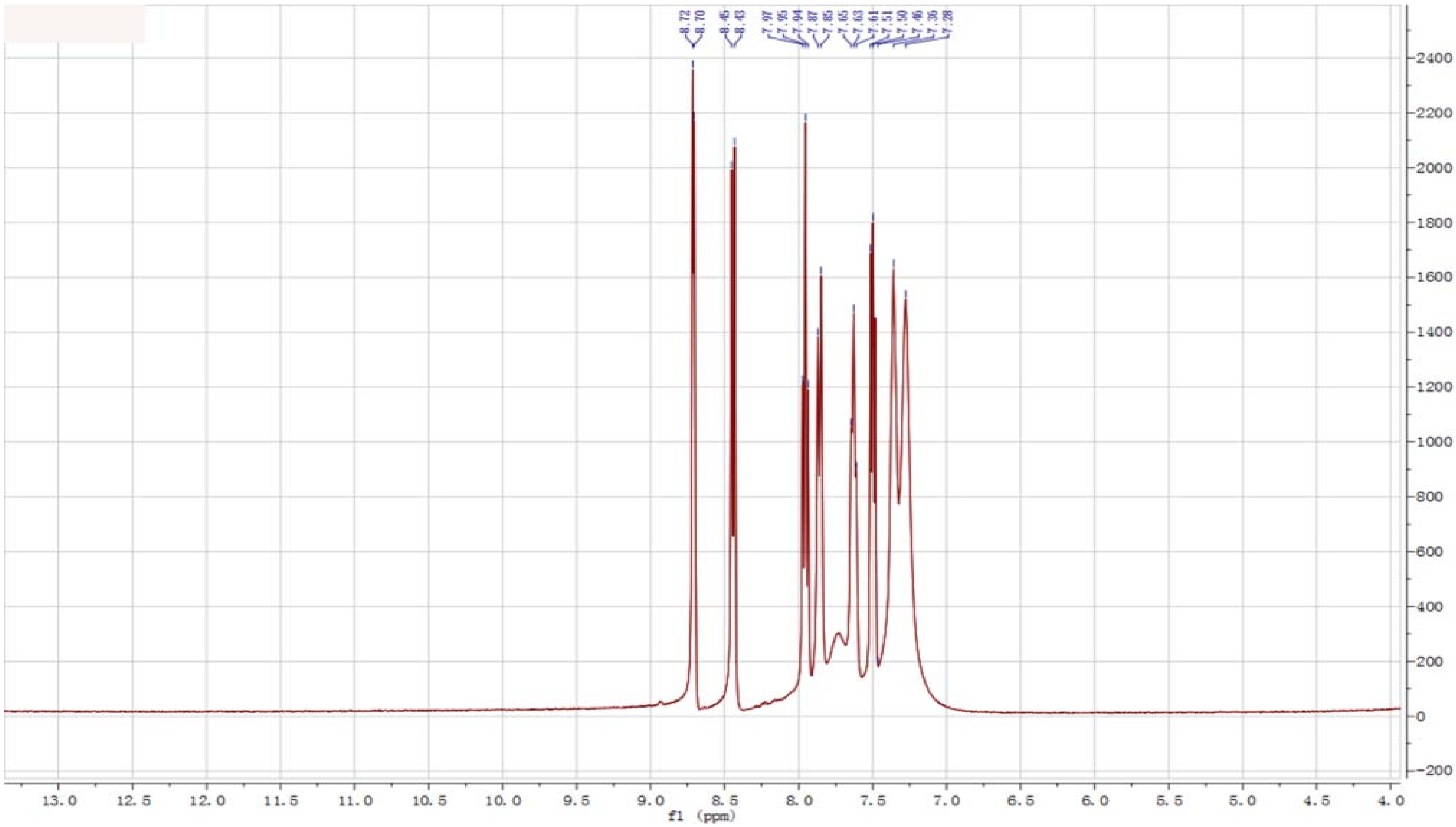

Figure S19. ^{1}H-NMR of **EuL-NH$_4$Cl** dissolved inDMSO-d^6.

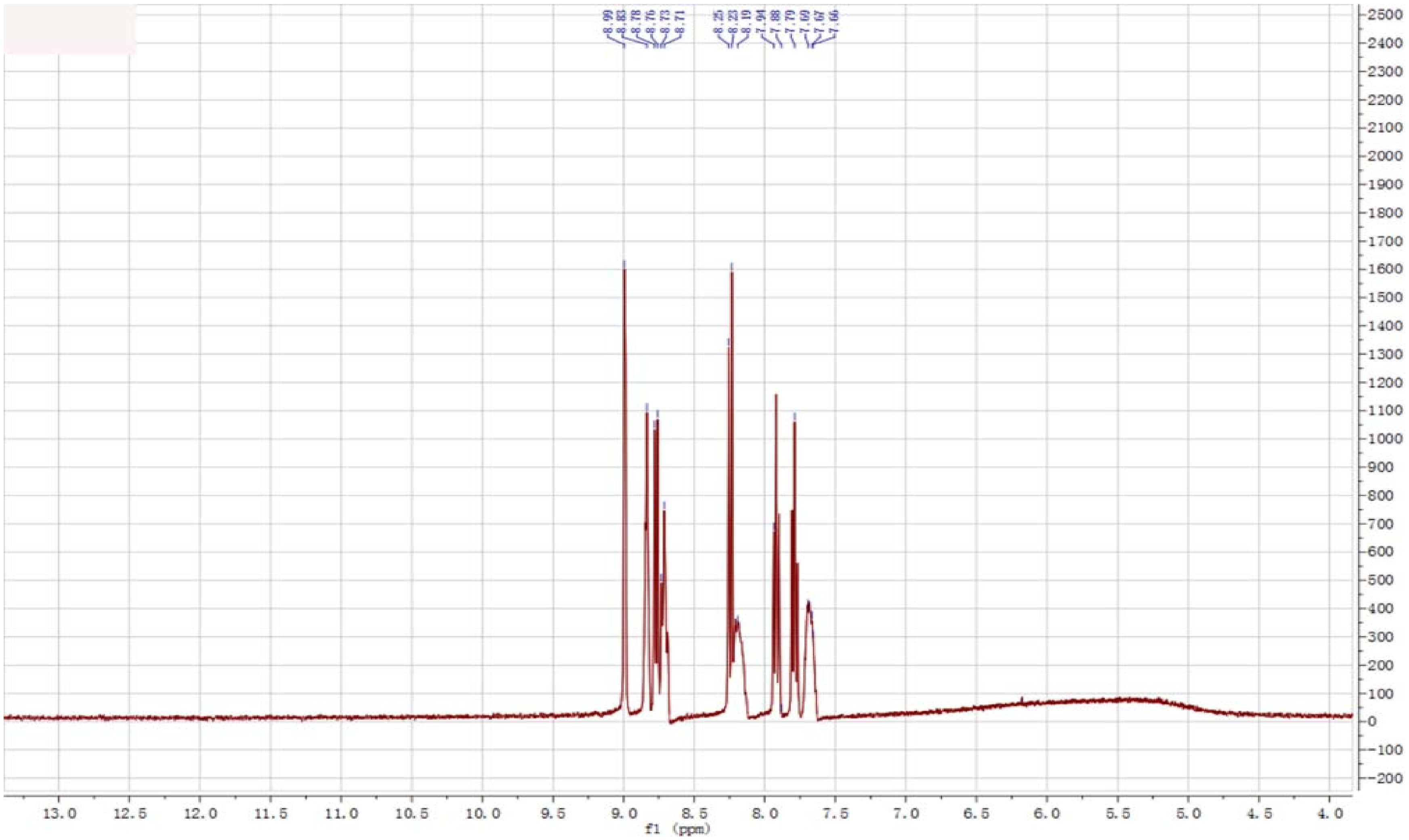

Figure S20. ^{1}H-NMR of **H_2LCl•H_2O** dissolved inDMSO-d^6.

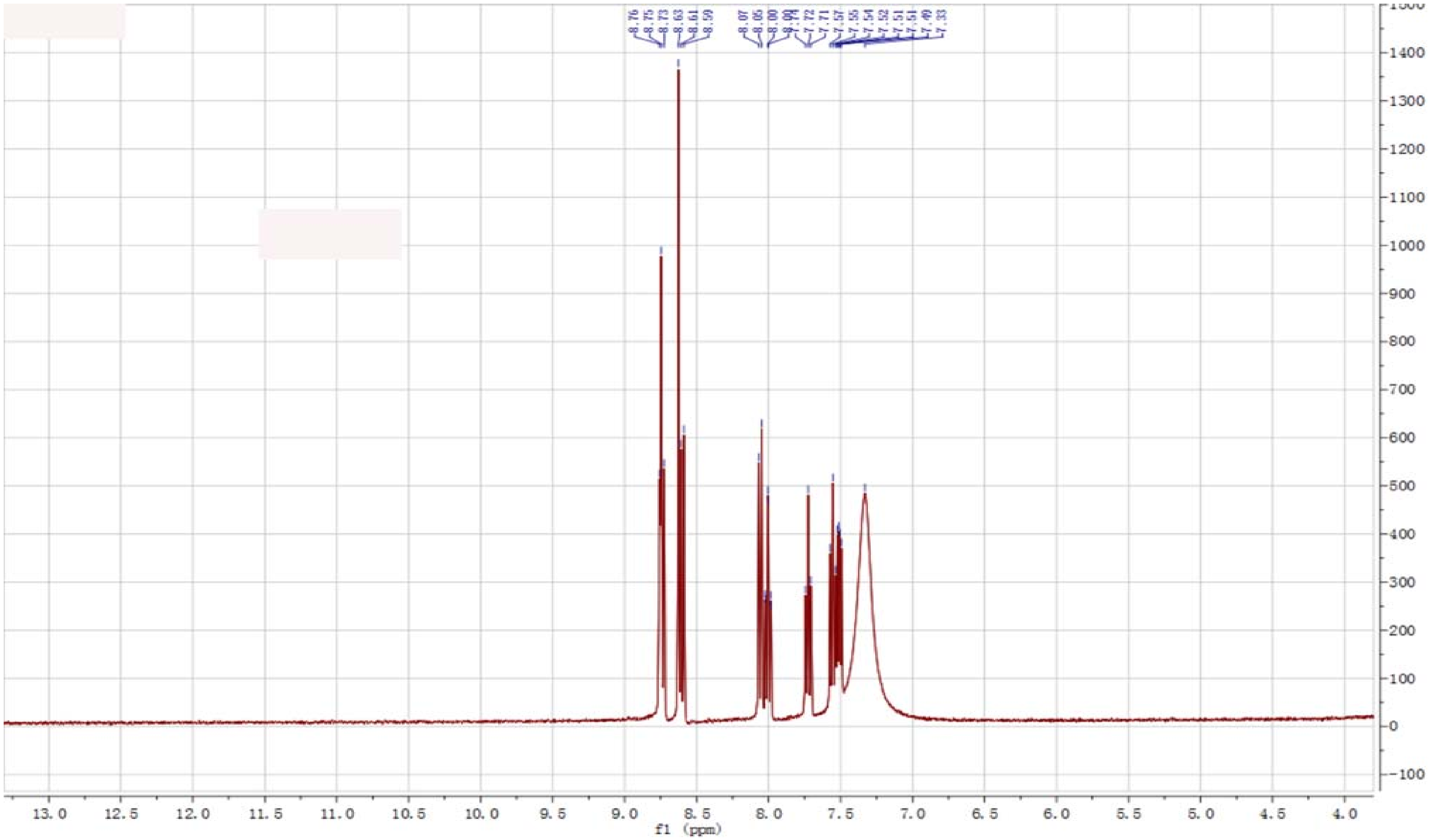

Figure S21. ^{1}H-NMR of **$H_2LCl{\bullet}H_2O$-NH_3** dissolved in DMSO-d^6.

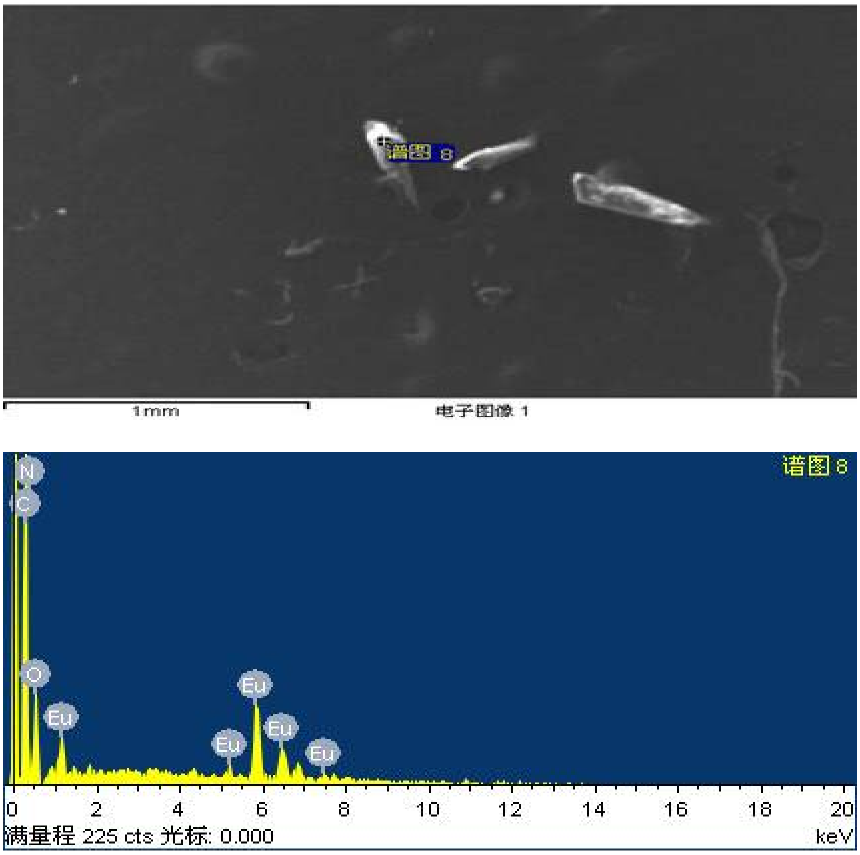

Figure S22. EDS of **EuL**.

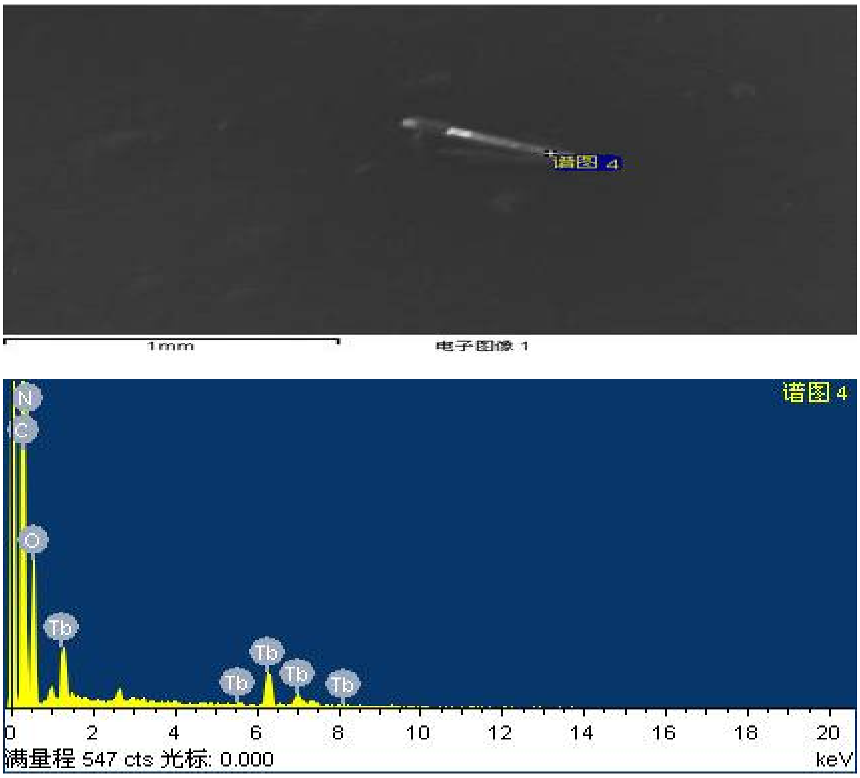

Figure S23. EDS of **TbL**.

Table S1. Crystallographic data of **EuL**, **TbL** and **$H_2LCl·H_2O$**.

compound	**EuL**	**TbL**	**$H_2LCl·H_2O$**
empirical formula	$C_{30}H_{19}EuN_6O_{10}$	$C_{30}H_{19}TbN_6O_{10}$	$C_{15}H_{13}ClN_2O_3$
formula weight	775.47	782.43	304.72
temperature (K)	100.00(13)	293(2)	99.98(18)
wavelength (Å)	0.71073	0.71073	1.54184
space group	*C*2/c	*C*2/c	*P* -1
Crystal syste	monoclinic	monoclinic	triclinic
a (Å)	17.4550(11)	17.400(5)	8.4489(7)
b (Å)	17.5918(9)	17.775(5)	8.9646(7)
c (Å)	19.7955(11)	19.987(6)	9.2306(5)
α (deg)	90	90	91.897(5)
β (deg)	104.960(7)	104.563(5)	97.303(5)
γ (deg)	90	90	95.599(6)
volume (Å^3)	5872.5(6)	5983(3)	689.42(8)
Z	8	8	2
D_c (Mg m^{-3})	1.754	1.737	1.468
μ (mm^{-1})	2.207	2.433	2.569
data collected	14157	24758	4490
unique data (R_{int})	5163	6842	2721
no. of param	424	424	198
GOF on F^2	1.047	1.024	1.045
R1^a [$I > 2\sigma(I)$]	0.0520	0.0618	0.0418
wR2^b	0.1498	0.1597	0.1086
^{a}R1 = $\sum||F_o| - |F_c||/\sum|F_o|$. ^{b}wR2 = $\{\sum[w(F_o^2 - F_c^2)^2]/\sum[w(F_o^2)^2]\}^{1/2}$.			

Table S2. The geometric data (Å, °) of hydrogen-bonds in **$H_2LCl·H_2O$**.

D–H···A	D–H	H···A	D···A	D–H···A
O19–H19···O1W$^{\#1}$	0.82	1.78	2.5819(19)	165.2
O1W–H1WA···Cl1$^{\#2}$	0.85	2.30	3.1445(15)	169.5
O1W–H1WB···Cl1	0.85	2.26	3.1141(17)	177.4
N1–H1···Cl1	0.85(3)	2.39(3)	3.1148(17)	143(2)

Symmetry codes: #1 -*x*+1, -*y*, -*z*+1, #2 -*x*+2, -*y*+1, -*z*+2

Table S3. The singlet and triplet energy levels of **$H_2LCl·H_2O$** and H**L** calculated by TDHF.

Compound	Excited states	Multiplicity	Excitation energy		Oscillator strength
			eV	cm^{-1}	
$H_2LCl·H_2O$	1	T	2.2811	18400	0
	2	T	3.3349	26900	0
	3	T	3.7780	30500	0
	1	S	4.2162	34000	0.1844
	2	S	4.5684	36800	0.3687
	3	S	5.4268	43800	0.6399
H**L**	1	T	2.6001	21000	0
	2	T	3.4002	27400	0
	3	T	3.7884	30600	0
	1	S	4.9557	40000	0.2171
	2	S	5.0850	41000	0.1176
	3	S	5.6586	45600	0.0102

1. S. Altobello, R. Argazzi, S. Caramori, C. Contado, S. Da Fré, P. Rubino, C. Choné, G. Larramona and C. A. Bignozzi, *J. Am. Chem. Soc.*, 2005, **127**, 15342-15343.
2. J. Chen, F. Y. Yi, H. Yu, S. Jiao, G. Pang and Z. M. Sun, *Chem. Commun.*, 2014, **50**, 10506-10509.
3. G. M. Sheldrick, *Acta Crystallogr. Sect. A: Found. Crystallogr.*, 2007, **64**, 112-122.